land

Article

Biodiversity of Woody Plant Species, Indicator Values and Soil Properties in Priority Habitat 91E0* in the Nestos Area, Greece: A Monitoring Study

Alexandra D. Solomou [1,*], Evangelia Korakaki [1], Christos Georgiadis [2], Panagiotis Michopoulos [1] and Georgios Karetsos [1]

[1] Institute of Mediterranean Forest Ecosystems (IMFE), ELGO-DIMITRA, Terma Alkmanos, Ilisia, 11528 Athens, Greece; ekorakaki@elgo.gr (E.K.); pmichopoulos@elgo.gr (P.M.); karetsos@fria.gr (G.K.)
[2] Department of Ecology, School of Biology, Faculty of Sciences, Aristotle University of Thessaloniki, 54124 Thessaloniki, Greece; gchristk@bio.auth.gr
* Correspondence: asolomou@elgo.gr

Abstract

Priority habitat 91E0* (alluvial forests with *Alnus glutinosa* and *Fraxinus excelsior*) constitutes a key riparian biodiversity hotspot, yet it is increasingly threatened by woody invasions that alter the community composition and reduce the habitat's heterogeneity. Ten permanent plots (15 m radius) were surveyed in the Nestos River delta (NE Greece) in 2019 and 2023, following a manual control campaign conducted in 2021, targeting *Amorpha fruticosa* and *Acer negundo*. Because systematic plot-level vegetation data were collected only in 2019 and 2023, the study evaluates before–after changes rather than continuous annual dynamics. Woody species composition and diversity, community turnover (Bray–Curtis dissimilarites/PCoA; PERMANOVA), invasive dynamics (negative binomial GLMs), and community-weighted Ellenberg-type indicator values and their relationships with the soil properties (0–30 cm) were assessed. Across the surveys, 18 woody taxa were recorded, dominated by native riparian trees and shrubs, together with four established alien species. The total alien abundance declined from 943 to 385 individuals between 2019 and 2023, driven by *A. negundo* (−68%) and *A. fruticosa* (−39%). The woody community composition differed significantly between years ($R^2 = 0.12$; $p = 0.013$) and river banks, whereas plot-scale diversity indices changed modestly and evenness increased. The mean community-weighted moisture affinity increased (CWM_F: 6.28 → 7.07), nutrient affinity remained high, and reaction values declined slightly. The soil's properties did not differ between the treated and control plots; nevertheless, Shannon diversity was positively correlated with organic C, total N, exchangeable Ca and K, and clay content. Permanent plot resurveys thatintegrate soil properties and indicator-based community metrics provide robust baselines to support Article 17 reporting under the EU Habitats Directive and to guide spatially targeted invasive-species management in Mediterranean alluvial forests (habitat 91E0) undergoing restoration actions.

Keywords: biodiversity; invasive alien species; *Amorpha fruticosa*; *Acer negundo*; soil properties; Nestos River

Check for updates

Academic Editor: Krish Jayachandran

Received: 31 December 2025
Revised: 6 February 2026
Accepted: 12 February 2026
Published: 15 February 2026

https://doi.org/10.3390/land15020335

1. Introduction

Riparian and floodplain forests are ecotonal habitats in which hydrology, sediment dynamics, and soil processes shape complex, dynamic plant communities that support high levels of biodiversity and key ecosystem functions [1–3]. In these environments, spatial and temporal variability in flow and flooding regimes directly influence the vegetation's composition and structure, generating gradients in soil moisture, nutrients, and texture [4–7]. These variations impact processes like regeneration, succession, and essential ecosystem services such as bank stabilization, nutrient retention, and habitat provision [5,6,8–10].

Under the EU Habitats Directive (92/43/EEC), habitat type 91E0* (alluvial forests with *Alnus glutinosa* and *Fraxinus excelsior*) comprises the remaining alder–ash alluvial forests and associated riparian communities, and is classified as a priority habitat type [11,12]. Its conservation status is considered particularly critical due to extensive degradation and fragmentation across its range [13]. The European monitoring guidance for 91E0* highlights that conservation status relies not just on the presence of species but also on functional attributes related to hydrological connectivity and sediment dynamics. These attributes include the regeneration capacity of native woody species, structural continuity, and the maintenance of hydro-edaphic heterogeneity, which sustains habitat mosaics and associated biodiversity [13].

In Greece, the Nestos River and its delta host the largest remaining tract of riparian forest in the country and are designated under the Natura 2000 network and the Ramsar Convention; the area is part of the National Park of Eastern Macedonia–Thrace (NP EMTH) [14,15]. The historical contraction of the Nestos floodplain forests, coupled with their current role as a regional biodiversity hotspot in the eastern Mediterranean, highlights the need for systematic, repeatable field-based monitoring capable of informing conservation reporting and management prioritization [14,15].

During the 20th century and continuing to the present, hydro-morphological alterations (channel straightening and levees) and, most notably, the construction and operation of the Thissavros and Platanovrysi reservoirs have substantially modified the flow regime, sediment supply, and the thermal/chemical signature of the downstream Nestos [16–18]. These changes have direct ecological consequences for riparian vegetation and alluvial forests dynamics, and they have also been documented through remote sensing approaches that capture pre- and post-impoundment shifts in vegetation indices [16–18]. However, field-based monitoring remains essential to translate hydro-morphological signals into vegetation responses, diagnose habitat condition, and identify management-relevant mechanisms at the plot scale.

At the same time, invasive alien plant species increasingly threaten habitat 91E0* along the Nestos River. A recent regional inventory documented the widespread occurrence of *Amorpha fruticosa* and other invasive woody taxa in the wider area, including *Acer negundo*, *Ailanthus altissima* (not recorded in our permanent plots) and *Robinia pseudoacacia* [19]. Because invasive woody plants can alter regeneration niches, competitive hierarchies, and stand structure, monitoring schemes must be sufficiently sensitive to detect early compositional shifts and to support timely, targeted management interventions, particularly where high-impact invaders are already established [19].

Despite the recognized sensitivity of alluvial forests to hydrological regulation and biological invasions, temporally explicit field evidence for Mediterranean occurrences of habitat 91E0* remains limited. Permanent plot resurveys provide a defensible basis for distinguishing short-term fluctuations from directional change, quantifying spatial turnover across hydro-edaphic gradients, and evaluating whether the control of invasive species coincides with measurable responses in native composition, diversity and diagnostic taxa [13,14].

From a regulatory standpoint, Article 17, reporting obligations under the Habitats Directive, and emerging EU forest monitoring initiatives make rigorous, repeatable assessments of habitat condition imperative, using indicators of composition, structure, and functions, and integrating soil and hydrological data [20,21]. These needs are aligned with broader EU efforts to strengthen and harmonize forest monitoring information (e.g., the Commission's proposed forest monitoring framework). Monitoring woody plant composition, alpha and beta diversity, and indicator values (community-weighted Ellenberg-type values) is particularly informative in habitats where small shifts in hydro-edaphic conditions entail disproportionate biotic responses. Moreover, the recent harmonization of European Ellenberg-type indicator values enables the consistent interpretation of plant assemblages along moisture, nutrient and soil reaction gradients across regions [22,23].

The aim of this study is to document the following within the Nestos sections of the priority habitat 91E0*: (a) spatiotemporal variability in woody plant composition and diversity; (b) the relationships between plant diversity and soil properties; (c) patterns in community-weighted Ellenberg-type indicator values as proxies for environmental gradients and habitat heterogeneity; and (d) the principal pressures associated with the observed changes. By integrating permanent plot resurveys with invasion metrics, soil properties, and indicator-based approaches, this study directly addresses current monitoring needs for Natura 2000 habitats in Greece and provides management-relevant indicators for assessing conservation status and planning targeted measures in Mediterranean alluvial forests.

2. Materials and Methods

2.1. Study Area

The alluvial forest of Nestos was one of the largest water-rich forests in the Mediterranean. At the beginning of the last century, it covered an area of 120,000 hectares and occupied almost 1/4 of the total area of the delta. Today, despite the fact that the forest is limited to approximately 8000 hectares, fragmentarily preserved on both sides of the river embankments, it remains the largest natural riparian forest in Greece in terms of extent, and is one of the most ecologically significant alluvial forest systems in Europe [24].

The study area is located in the north-eastern part of Greece, within SCI GR1150010 (a Natura 2000 site). It includes alluvial forests of the priority habitat 91E0* in the Nestos Delta (Figure 1). The Nestos River, which is also called the Mesta River in Bulgaria, is about 234 km long, with about 130 km in Greece. It flows into the Aegean Sea. The river forms a natural border between Greece and Bulgaria, and represents one of the most important fluvial systems for biodiversity in the Balkans. Its floodplain supports extensive alluvial forests, shaped by hydrological dynamics. This makes them a unique habitat for many different plants and animals [25].

According to the UNEP Climate Zone Classification System, the Nestos Delta falls within a humid to sub-humid Mediterranean climatic zone [26]. Its designation as both a Ramsar wetland and a Natura 2000 site reflects the relatively high annual precipitation and river discharge that sustain wetlands, reed beds, lagoons, and riparian forests. These conditions make the delta particularly important for diverse flora and fauna, including migratory bird populations. However, the last 50 years of climatic assessments in the region brought to the fore a spatial redistribution of precipitation in the deltaic system [27]. A significant observation is the decline of rainfall in the delta's coastal zone, specifically in the alluvial forest section.

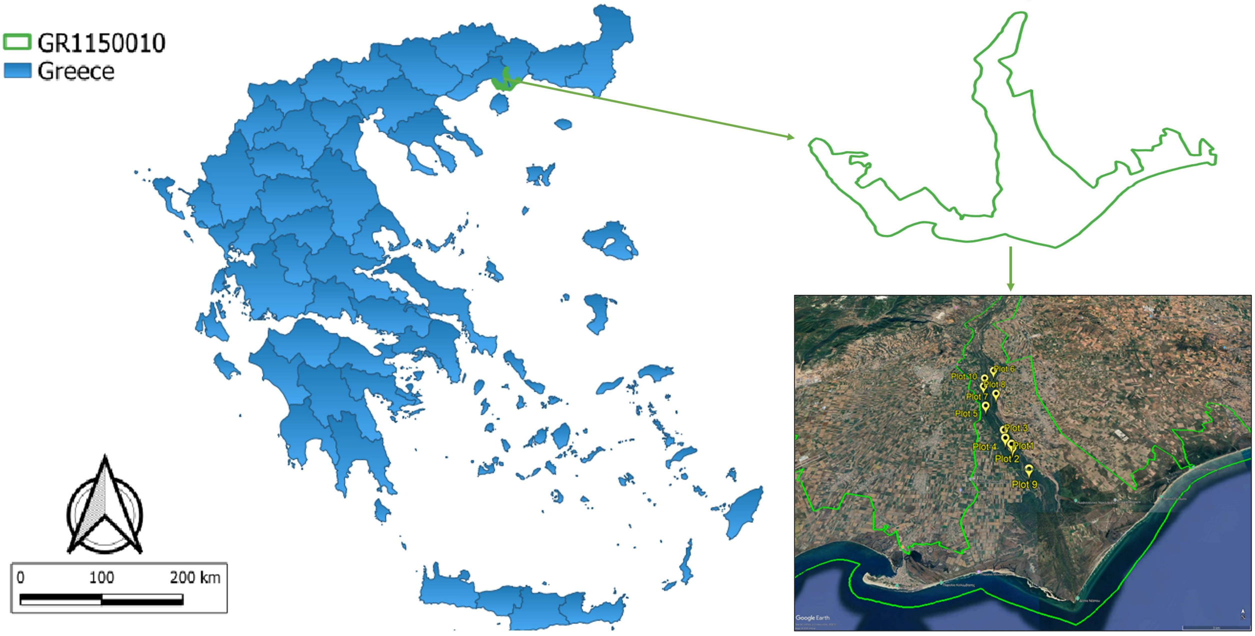

Figure 1. Study area in Greece. Yellow markers indicate permanent sampling plots.

2.2. *Plot Establishment and Management Intervention*

Ten (10) circular permanent plots (Plot 1–10), each with a radius of 15 m, were established in May 2019. They were randomly and homogeneously distributed along the habitat [3]. The plots' numbering reflects their order of establishment during fieldwork and does not strictly follow a north–south sequence; however, the spatial arrangement of the plots along the river corridor (including upstream–downstream and east–west positioning) is explicitly shown in Figure 1 and was considered in the analyses (e.g., by including the river bank as a factor). Furthermore, during the summer of 2021, individuals of *A. fruticosa* and *A. negundo* were manually cut in all ten permanent plots.

The intervention consisted of manually cutting the aboveground biomass at the ground level without any chemical treatment and implemented uniformly in all plots. No root or soil manipulation was carried out. This management belongs to local conservation measures and is a major disturbance between the two surveys (2019 and 2023).

2.3. *Vegetation Sampling*

Woody Plants

The data collection was conducted in May 2019 across ten plots. Within each plot, the composition, abundance and the number of woody plant species were recorded. Similar measurements carried out across the same ten plots in May 2023 and were used for comparative analysis. More specifically, vegetation studies were conducted in 2019 (pre-intervention) and repeated in 2023 (post intervention). No systematic plot-level data were collected in the intervening years (2020–2022), and therefore the present study focuses on before–after comparisons rather than continuous annual dynamics.

2.4. *Soil Sampling and Analyses*

In July 2023, soils were sampled to evaluate potential short-term effects of invasive woody removal on topsoil properties. The ten permanent plots (treated in 2021) were sampled and compared with ten adjacent, unmanaged plots used as controls. In each of the 20 plots, two soil samples were collected from 0 to 30 cm depth at two positions within the plot, and the two samples were analyzed separately. This yielded 20 samples from the treated plots and 20 samples from the control plots ($N = 40$) in the riparian forest.

All soil samples were air dried and passed through a 2 mm sieve. The subsamples of sieved soils were pulverized in a ball mill for the determination of organic C, calcium carbonate and Kjeldahl N. The texture of the soils was determined by the hydrometer method [28], while the $CaCO_3$ content was measured by a calcimeter based on the reaction of $CaCO_3$ with HCL. The pH of the soils (1:2.5 soil: water; ratio per weight) was measured by a glass electrode. The conductivity of the soil solution was determined using a conductivity meter in a soil aqueous solution (1:5 soil: water; ratio by weight after one hour of shaking) and the result was multiplied by 6.4 [29]. Exchangeable cations (Ca, Mg, K and Na) were extracted with 1 M of NH_4–acetate solution at pH 7, and the organic C content was determined with the potassium dichromate ($K_2Cr_2O_7$) method [30]. Organic N, together with the ammonium N, the so called Kjeldahl N, was extracted with concentrated sulfuric acid (H_2SO_4) and the concentration of each was determined with the Kjeldahl distillation method [31].

2.5. Plant Diversity and Functional Diversity Analyses

Plant diversity was assessed using species richness (S), Shannon diversity (H′), Simpson diversity (1-D) and Pielou's evenness (J′) [32,33]. All indices were calculated with the Species Diversity and Richness IV, version 4.1.2 (Pisces Conservation Ltd., UK) [34].

Statistical analyses were conducted in R Version 4.2.0 (R Core Team, 2022) [35]. The permanent plot dataset comprised ten circular plots (15 m radius) surveyed in 2019 and resurveyed in 2023 (paired design; 20 plot–year samples). Woody abundance data comprised stem counts per plot and year. Unless stated otherwise, statistical significance was assessed at alpha = 0.05.

Functional diversity and functional composition: Functional diversity was quantified with Rao's quadratic entropy (Q) and functional dispersion (FDis) using a trait matrix (growth form: tree/shrub/liana; origin: native/alien; and nitrogen-fixing ability: yes/no) and plot–year relative abundances (FD and dbFD). Temporal changes in Q and FDis were tested with linear mixed effects models (year fixed; plot random intercept). The proportions of alien individuals and nitrogen-fixing individuals were analyzed using binomial generalized linear mixed models, with the number of alien (or nitrogen-fixing) stems modelled as successes out of the total number of stems per plot–year (logit link), including year as a fixed effect and plot as a random intercept.

2.6. Community Composition and Beta Diversity

A species-by-sample matrix (20 plot–year samples) was assembled from stem counts. Abundances were converted to within-sample relative abundances and Hellinger-transformed (square root of relative abundance) abundances to down weight the dominant taxa and reduce the influence of joint absences. Bray–Curtis dissimilarities were computed and visualized using principal coordinates analysis (PCoA).

Incidence-based Sorensen beta diversity (betaSOR) and its turnover (betaSIM) and nestedness-resultant (betaSNE) components were computed with betapart and summarized for (i) pairwise comparisons among plots within each year and (ii) temporal comparisons of the same plot between 2019 and 2023.

2.7. Statistical Analyses

PERMANOVA and dispersion diagnostics: Effects of year, river bank (East/West), invasion intensity and soil gradients on community composition were tested with PERMANOVA (adonis2 in vegan) on Bray–Curtis dissimilarities. The invasion intensity was quantified as the combined stem count of *Acer negundo* and *Amorpha fruticosa* per plot–year (counts per plot); counts were log1p-transformed and standardized prior to analysis. The Soil conditions were represented by the first two axes of a PCA on standardized soil variables (Soil_PC1 and Soil_PC2; see below. $CaCO_3$ excluded from the PCA due to missing values). Because plots were resurveyed (paired design), permutation tests were constrained within plots (strata = Plot; 999 permutations). The homogeneity of multivariate dispersions for year and bank groups was assessed with betadisper followed by permutest (999 permutations).

Models for invasive alien woody abundance: Temporal and environmental controls on invasive abundance were analyzed separately for *Acer negundo*, *Amorpha fruticosa* and *Morus alba*. The responses were the stem counts per plot–year; therefore, negative binomial generalized linear mixed models with a log link function were fitted with year, bank, Soil_PC1 and Soil_PC2 as the fixed effects, and plot as a random intercept (e.g., glmmTMB). The model adequacy was evaluated using residual simulation diagnostics (DHARMa) and checks for overdispersion and zero inflation. The results are reported as log-scale coefficients and as incidence rate ratios (exp(beta)) with 95% confidence intervals.

Indicator values: Community-weighted mean (CWM) Ellenberg-type indicator values for moisture (F), nutrients (N) and reaction (R) were calculated for each plot–year as abundance-weighted means using the harmonized European dataset [23]. Temporal shifts in CWM_F, CWM_N and CWM_R were tested with linear mixed effects models (year fixed; plot random intercept). The Associations between CWMs, soil gradients, Shannon diversity and invasive abundance were evaluated using mixed effects models with plot as a random intercept; Pearson correlations are reported for descriptive purposes.

Soil properties: For each soil parameter, we calculated the coefficient of variation (CV, %, 100 × SD/mean) and the range of observed values (minimum–maximum) within each treatment group. There were two treatments. One control and the other with the alien plants removed. The soil properties were compared through an Analysis of Variance Test (ANOVA). Due to the high variability of the values of soil properties, there was logarithm conversion of all values with the exception of that pH which is already a logarithm. Also, the Pearson correlation coefficients were employed to account for the correlations between the soil properties measured and Shannon plant diversity index in the plots. Soil analyses were conducted in IBM SPSS Statistics (Version 26.0) [36].

3. Results

3.1. Woody Plant Composition at Nestos River Sites

Tables S1–S21 (Supplementary Material) lists 18 woody taxa (13 families) recorded across the study area over the two survey years (2019 and 2023). The tree and shrub layer is dominated by native, non-range-restricted (i.e., widespread) taxa (14 of 18). These include characteristic riparian trees such as *Salix alba*, *Populus alba* and *P. nigra* (Salicaceae), *Alnus glutinosa* (Betulaceae) and *Fraxinus angustifolia* (Oleaceae). Chorologically, European–SW Asian and Mediterranean–European elements predominate, accompanied by Euro-Siberian, east Mediterranean, Mediterranean and Mediterranean–SW Asian elements (Supplementary Table S1), indicating mixed biogeographic affinities of the riparian woody flora.

At the same time, four alien established species were recorded: *Acer negundo*, *Amorpha fruticosa* and *Robinia pseudoacacia* (of North American origin) as well as *Morus alba* (of East Asian origin). Although *Ailanthus altissima* has been reported for the wider Nestos riparian zone [19], it was not recorded in any of the permanent plots surveyed in 2019 or 2023 (Table S1). The presence of alien taxa indicates anthropogenic pressure and ongoing invasion dynamics, without overriding the dominance of native species. The recorded woody taxa were *Acer negundo*, *Alnus glutinosa*, *Amorpha fruticosa*, *Celtis australis*, *Cornus sanguinea*, *Ficus carica*, *Fraxinus angustifolia*, *Morus alba*, *Periploca graeca*, *Populus alba*, *Populus nigra*, *Prunus cocomilia*, *Quercus robur*, *Robinia pseudoacacia*, *Rubus sanctus*, *Salix alba*, *Sambucus nigra* and *Ulmus minor* (Supplementary Table S1). All the recorded taxa belonged to the phanerophyte life form (Supplementary Table S1), confirming that the woody vegetation is dominated by trees and large shrubs typical of riparian zones.

Overall, the species composition indicates a mature riparian woody community, with a strong core of native European/Mediterranean elements, but enriched locally by established alien species that need monitoring in terms of their spread and ecological impact.

According to Figure 2, the percentage distribution of taxa by family (richness based) reflects how the number of woody species is distributed among the plant families in Nestos per year. In 2019, taxa from 12 families were recorded, with higher representation in Salicaceae, Moraceae and Rosaceae (each 13.3% of total taxa). The remaining families (Fabaceae, Adoxaceae, Sapindaceae, Betulaceae, Apocynaceae, Cornaceae, Cannabaceae, Oleaceae and Ulmaceae) were represented by a single taxon each (6.7%), indicating a relatively even family-level structure without a single strongly dominant family. In 2023, the total family richness increased to 13 due to the emergence of Fagaceae (5.6% of taxa). Salicaceae remained the wealthiest family and was slightly boosted (16.7%) while Moraceae and Rosaceae each accounted for 11.1%. Fabaceae also increased to 11.1% in 2023. The remaining families (Adoxaceae, Sapindaceae, Betulaceae, Apocynaceae, Cornaceae, Cannabaceae, Oleaceae and Ulmaceae) each contributed 5.6%. Overall, the small percentage shifts between years mainly reflect changes in the total number of recorded taxa and the addition of one family in 2023, rather than loss of families from the community.

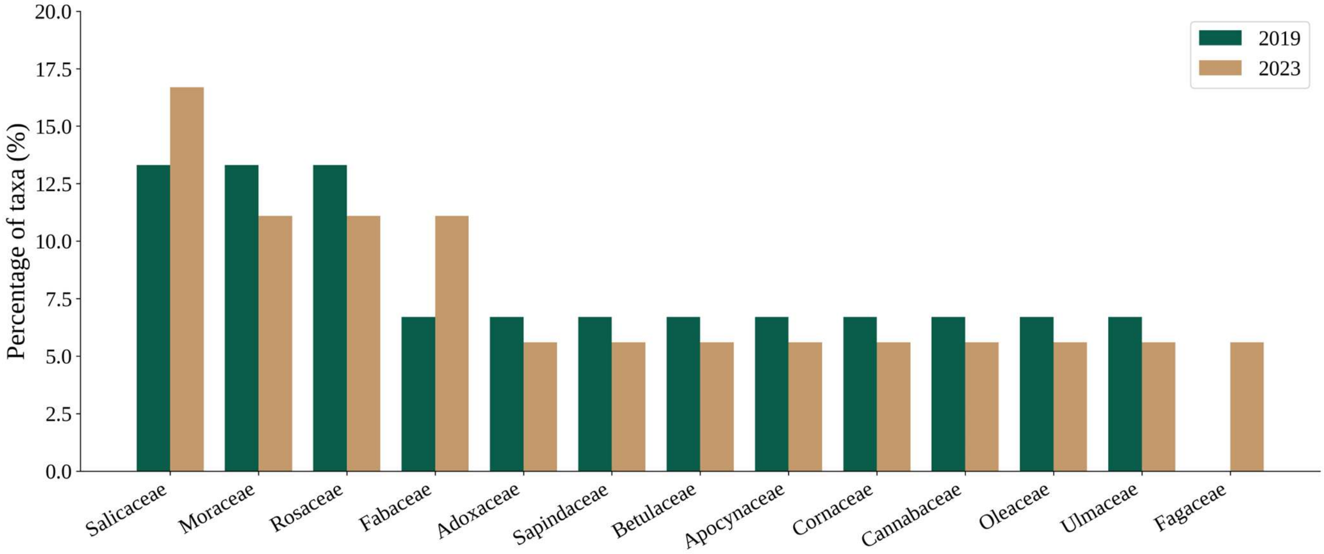

Figure 2. Percentage distribution of plant species across plant families in Nestos River sites (2019 and 2023).

3.2. Dynamics of Invasive Woody Species at the Plot Scale

The spatial and temporal distribution (2019 vs. 2023) of the below alien woody species (Figure 3): In total, four alien woody species were recorded in the permanent plots (*Acer negundo*, *Amorpha fruticosa*, *Morus alba* and *Robinia pseudoacacia*). In general, the woody alien abundance decreased significantly over time, dropping from a total of 943 plants in 2019 to 385 in 2023 (approximately 60% reduction). This decrease is mainly induced by *Acer negundo* and *Amorpha fruticosa*, the two most dominant invasion alien species in the study area, and that have been detected for manual treatment on purpose between the two surveys. In contrast, *M. alba* had low (with slight increase) and *R. pseudoacacia* extremely low densities, and, as such, a weak momentum of invasion during the study period. This pronounced reduction can be attributed to the combined effect of management actions and population structure. In both survey years, we counted all individuals recorded within the permanent plots, including mature trees as well as saplings and juvenile individuals, following the same field protocol; therefore, the decline is not a methodological artefact. Field observations suggest that the decrease is chiefly related to removal and heavy reduction in juvenile and sapling cohorts of *A. negundo* and *A. fruticosa*, which were especially numerous in 2019. The decline in the number of mature individuals, however, was less pronounced, such that the dramatic decrease in young individuals contributes significantly to the approximately 60% overall reduction in total alien abundance between 2019 and 2023.

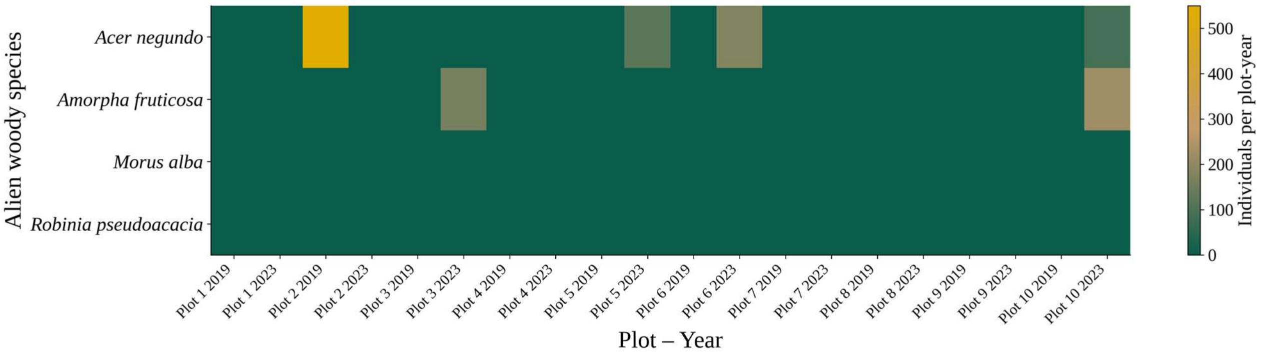

Figure 3. Heatmap showing the spatial and temporal distribution of alien woody species (including both invasive and naturalized taxa) recorded in the permanent plots in 2019 and 2023 (*Acer negundo*, *Amorpha fruticosa*, *Morus alba* and *Robinia pseudoacacia*).

Morus alba, a naturalized alien species in the study area (not considered invasive in Greece), occurred at low but increasing densities (seven individuals in 2019 vs. seventeen in 2023), most frequently in Plots 5 and 7. *Robinia pseudoacacia*, a commonly planted but potentially invasive alien tree, was almost absent from the study plots (one individual in Plot 3 in 2023). *Ailanthus altissima*, although reported in the wider Nestos riparian zone, was not recorded in any permanent plot in either year, and is therefore not included in the plot-based counts. Overall, the heatmap indicates a pronounced reduction in the dominance of the two main invaders (*Acer negundo* and *Amorpha fruticosa*), a partial spatial shift in invasion hotspots driven by these two invaders among plots, and the sparse but increasing presence of *M. alba*, with *R. pseudoacacia* currently having only a minor influence on the local alien species pool. *Acer negundo* is the dominant alien taxon in both years and appears as the most intense band in the heatmap. In 2019 it reached very high densities in Plot 2 (583 individuals) and contributed substantially in Plots 5, 9, 1, 4 and 10. By 2023, its abundance had decreased from 703 to 225 individuals overall (~68% reduction), and high values shifted towards Plots 6, 3 and 9, while the strongly invaded Plot 2 showed much lower densities. *Amorpha fruticosa* exhibits a comparable pattern: while in 2019 it is primarily (>198) centred around Plot 10 and to a lesser extent Plot 9, in 2023 the main site hotspot lies in Plot 3 (115 individuals). Given this redistribution, the aggregate count of *A. fruticosa* individuals dropped from 233 to 142 (~39% decrease).

Morus alba occurred at low densities but increased over time (7 individuals in 2019; 17 in 2023), mainly in Plots 5 and 7. *Robinia pseudoacacia* was nearly absent, with only one record (Plot 3, 2023). *Ailanthus altissima*, though reported from the broader Nestos riparian zone, was not detected in any permanent plot in either year and is not included in plot-based counts. The heatmap therefore reflects both a pronounced contraction of *Acer negundo* and *Amorpha fruticosa* and a concurrent, low-level rise of *M. alba*.

3.3. Woody Plant Diversity

Table S22 (Supplementary Material) shows the diversity of woody plants in all permanent sampling plots for the years 2019 and 2023. For each plot, the species number (S), and the Shannon (H), Simpson (1–D) and Pielou index (J) are recorded. Between the two years there are variations in both species richness and population structure. In plots 3, 6 and 10, species richness, and Shannon and Simpson indices increase, suggesting an improvement in diversity and the distribution of abundance among the species. In contrast, in plots 1, 2, 4 and 7, species richness decreased between 2019 and 2023. However, in some cases (e.g., Plot 2), the Shannon and Simpson diversity indices increased, indicating that the reduction in the species number was mainly associated with the loss of rare or sporadically occurring species, while the relative abundances of the remaining species became more evenly distributed. The Pielou index (J) shows an increase in several plots (1, 2, 3, 4, 7, 8, and 10), indicating a general trend toward the more uniform participation of species in the woody community in 2023.

The functional diversity was analyzed in terms of the Q value of Rao's quadratic entropy index according to the growth form (tree/shrub/Liana), ancestry (native/alien) and capacity of the nitrogen fixation species (Supplementary Table S23). At the total surface level, the average Rao's Q value increased from 0.27 in 2019 to 0.34 in 2023, indicating an increase in the functional diversity of woody plant communities, expressed as greater trait dissimilarity among co-occurring species. Characteristic is the marked increase in Q on surfaces 2, 3, 6 and 10, where the reinforcement of nitrogenous species and the mixing of different growth forms led to more functionally heterogeneous compositions. In contrast, on surfaces 5, 8 and 9, Rao's Q declined, as a result of the dominance of a few functionally similar species. Although the number of species per surface area remained almost constant, the share of nitrogen-binding species increased from ~20% to ~39%, while the relative abundance of alien species decreased from ~47% to ~28%, indicating a shift in functional composition.

As a complementary indicator of functional diversity, the FDis (functional dispersion index), which reflects an abundance-weighted measure of the mean distance (trait) shown by species to their community centroid in multivariate trait space, was calculated (Supplementary Tables S24 and S25). The average FDis value per plot rose from 0.62 in 2019 to 0.77 in 2023, suggesting that higher dispersion (i.e., abundance-weighted differentiation between the considered traits) of woody communities across time.

The largest increases were observed in Plots 2, 3, 6 and 10 (and to a lesser extent in Plots 1 and 4), consistent with a higher relative representation of nitrogen-fixing taxa and a broader mixture of growth forms (trees, shrubs and lianas) and origins (native vs. non-native) within these plots. Conversely, FDis decreased in Plots 8 and 9 (and to a lesser extent in Plots 5 and 7), indicating reduced dispersion in trait space (functional homogenisation) associated with the dominance of fewer functionally similar taxa. Overall, the patterns in FDis were broadly concordant with Rao's Q, supporting that measurable shifts in functional composition occurred between 2019 and 2023.

3.4. Multivariate Patterns of Woody Plant Composition

The PCoA ordination of woody species composition, based on Bray–Curtis dissimilarities of Hellinger-transformed abundances, revealed a moderate but clear temporal signal (Figure 4). The first and second axes showed that the total diversity of community plant composition was represented by 27.0% and 19.8%, respectively, and they together accounted for 46.8%. Most of the 2019 samples showed more positive scores on the second axis, while 2023 samples generally moved towards negative PCoA2 scores. This indicates that there was a change in the composition of woody species over the years. The variations in spacing between the river banks were not very apparent and were mostly exhibited along PCoA1, with the east bank plots having somewhat more negative scores than the west bank plots. The woody community composition differed significantly between years and PERMANOVA confirmed this (year: $R^2 = 0.12$, pseudo-$F_{1,14} = 2.51$, and $p = 0.013$; Table 1), and to a lesser extent, between river banks (bank: $R^2 = 0.06$, pseudo-$F_{1,14} = 1.25$, and $p = 0.034$). In contrast, the intensity of invasion, expressed as the combined abundance of *Acer negundo* and *Amorpha fruticosa* per plot and year, had no significant effect on community composition at the current level of spread (Invader_abundance: $R^2 = 0.04$, pseudo-$F_{1,14} = 0.73$, and $p = 0.106$). The two principal soil gradients, summarized by Soil_PC1 and Soil_PC2, each explained only a small proportion of the variance in woody community composition ($R^2 = 0.03$–0.04; $p \geq 0.20$), even though Soil_PC1 and Soil_PC2 together captured 61.8% of the variability in the underlying soil dataset (42.39% and 19.39% of the variance, respectively; Supplementary Table S26). Finally, the full model explained roughly 29% of the variation in woody species composition among plots and years, with approximately 71% remaining unexplained. This unexplained variance is likely attributable to unmeasured fine-scale drivers that are known to structure riparian vegetation, including microtopography and small differences in elevation relative to the active river channel, hydrological conditions (e.g., flooding frequency and duration, and groundwater depth), sediment deposition and erosion patterns, and local disturbance events (e.g., tree-fall gaps and selective cutting). Furthermore, stochastic recruitment and mortality mechanisms, historical disturbance legacies, and biotic interactions may influence compositional variations among plots. These factors can vary markedly over short distances in alluvial forests and were not captured by the plot-level soil chemistry and invasion metrics measured in this study.

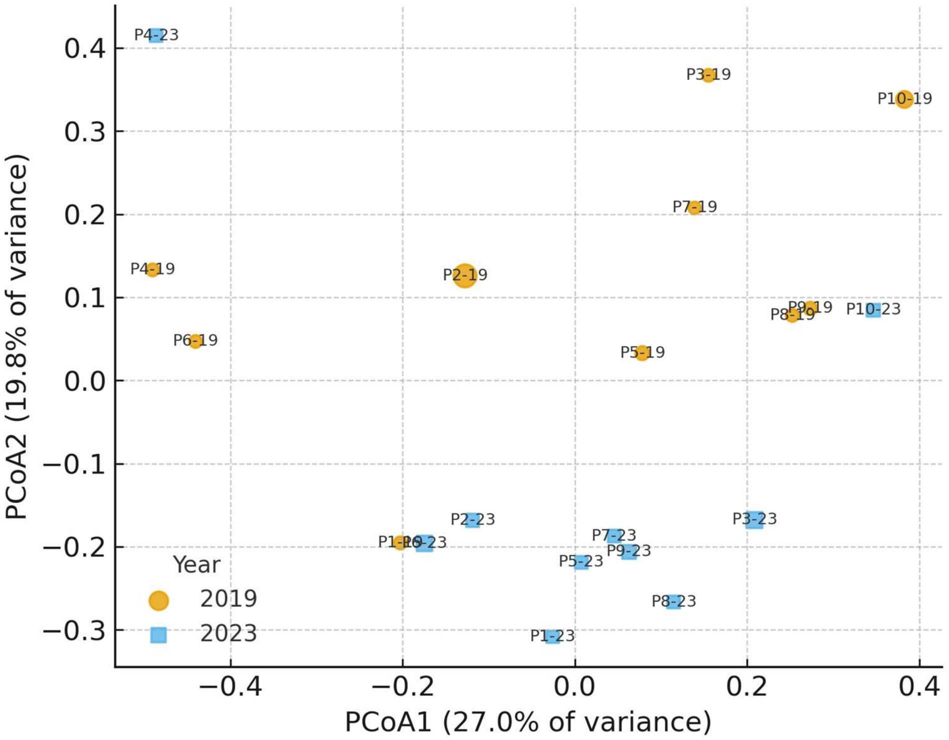

Figure 4. Principal coordinates analysis (PCoA) ordination of woody species composition in the ten permanent plots along the Nestos River, sampled in 2019 and 2023. The ordination is based on

Bray–Curtis dissimilarities computed from Hellinger-transformed species abundances. Circles represent samples from 2019 and squares represent samples from 2023. Labels denote plot identity and year (e.g., "P1-19" for Plot 1 in 2019). Point size is proportional to the combined abundance of the two invasive alien woody species (*Acer negundo* + *Amorpha fruticosa*) per plot and year. The first two axes explain 27.0% and 19.8% of the total variation in community composition, respectively.

Table 1. PERMANOVA results for woody species composition (Bray–Curtis dissimilarities of Hellinger-transformed abundances) in ten permanent plots sampled in 2019 and 2023.

Factor	df	SS	R^2	Pseudo-F	*p* (999 Perm.)
Year	1	0.537	0.123	2.51	0.013
Bank	1	0.264	0.06	1.25	0.034
Invader_abundance	1	0.157	0.036	0.73	0.106
Soil_PC1	1	0.148	0.034	0.68	0.203
Soil_PC2	1	0.184	0.042	0.83	0.298
Residual	14	3.093	0.706	–	–
Total	19	4.381	1	–	–

3.5. Beta Diversity and Species Turnover Between Years

The time-wise comparisons of the same plot between 2019 and 2023 demonstrated moderate beta diversity (mean β SOR = 0.34 ± 0.22) with, once again, a strong emergence of species turnover (β SIM = 0.24 ± 0.21) relatively to pure nestedness (β SNE = 0.10 ± 0.11). This pattern indicates that temporal changes were driven primarily by the replacement of species rather than by systematic species loss (Figure 5).

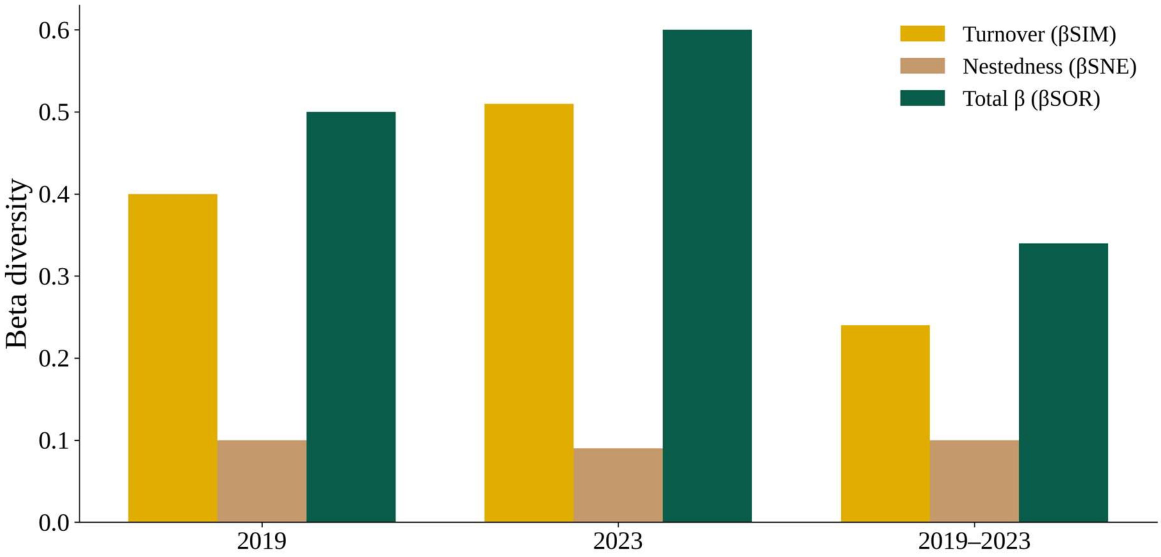

Figure 5. Partitioning of Sørensen beta diversity [16] for woody plant assemblages along the Nestos River. Bars show mean values of total beta diversity (βSOR), its turnover component (βSIM) and nestedness-resultant component (βSNE) for (i) pairwise comparisons among plots in 2019. (ii) Pairwise comparisons among plots in 2023, and (iii) temporal comparisons of the same plot between 2019 and 2023. In all cases, beta diversity is dominated by species turnover, whereas the nestedness component is relatively small.

The plots presented divergent temporal trajectories; for instance, Plot 3 and Plot 4 were strongly subject to yearly swapping (βSOR ≥ 0.60 βSIM ≥ 0.50), while the plot-scale turnover among woody species was practically nil in Plot 10 (βSOR = 0). Temporal changes in the relative abundance of the two main invasive alien woody species (*Acer negundo* and *Amorpha fruticosa*) showed a positive but non-significant association with temporal beta diversity (βSOR vs. Δinvader relative abundance: r = 0.55 and *p* = 0.10; βSIM vs. Δinvader relative abundance: r = 0.41 and *p* = 0.24). This pattern suggests a weak association: plots that experienced larger shifts in invader abundance generally diverged more from the initial community, although this was not statistically supported in this dataset.

3.6. Invasion Dynamics and Environmental Controls

The results from Negative Binomial GLMs showed that the abundance of both IAS trees declined significantly in agreement with observed data between 2019 and 2023 regardless of the river bank and soil conditions, (Tables 2 and 3). Compared to 2019, the average stem density for *Acer negundo* in 2023 was 69% lower (year effect: β = −1.17 ± 0.49 SE, z = −2.37, and *p* = 0.018), and it was approximately 70% lower for *Amorpha fruticosa* (β = −1.19 ± 0.51 z = −2.32, and *p* = 0.021). In both cases, invasion intensity increased along the first soil principal component (Soil_PC1), with *Acer negundo* and *Amorpha fruticosa* being 1.6-fold and 1.5-fold more common per unit increase in Soil_PC1 ($p \leq 0.003$), indicating a preference for relatively fertile, base-rich, or more disturbed sites. By contrast, *Morus alba* did not show a significant temporal trend (year: *p* = 0.43). It was, however, negatively associated with Soil_PC1 (β = −0.47 ± 0.18, z = −2.55, and *p* = 0.011) and was more abundant in plots characterized by more degraded or less altered soils (Table 4). River bank effects were not significantly related to *Acer negundo*, but *Amorpha fruticosa* was negatively correlated with the river in a significant way (β = −1.64 ± 0.69 z = −2.37, and *p* = 0.018), similarly to heatmap patterns across the east bank. Overall, the models indicate that while the temporal dynamics of invasive woody species were strongly influenced by management-related year effects and soil gradients, river bank effects were species specific.

Table 2. Coefficients of the negative binomial generalized linear model (GLM) for *Acer negundo* stem counts per plot and year. The response variable is the number of *A. negundo* individuals per plot in each sampling year (2019, 2023). Fixed effects include sampling year (year: 2023 vs. 2019), river bank (bank: east vs. west) and the first two principal components of soil conditions (Soil_PC1 and Soil_PC2). Estimates (β) are on the log scale. The year was coded as 0 = 2019 and 1 = 2023, and the bank as 0 = west and 1 = east. CI = 95% Wald confidence interval.

Predictor	Estimate (β)	Standard Error	z-Value	*p*-Value	95% CI (Lower)	95% CI (Upper)
Intercept	3.62	0.36	10.10	<0.001	2.92	4.33
Year (2023 vs. 2019)	−1.17	0.49	−2.37	0.018	−2.14	−0.20
Bank (East vs. West)	0.12	0.62	0.19	0.849	−1.10	1.34
Soil_PC1	0.48	0.12	4.09	<0.001	0.25	0.71
Soil_PC2	0.12	0.17	0.73	0.466	−0.21	0.46

Table 3. Coefficients of the negative binomial generalized linear model (GLM) for *Amorpha fruticosa* stem counts per plot and year. The response variable is the number of *A. fruticosa* individuals per plot in each sampling year. Fixed effects are the same as in Table 2 year (2023 vs. 2019), bank (east vs. west), and Soil_PC1 and Soil_PC2. Estimates (β) are expressed on the log scale. The year was coded as 0 = 2019 and 1 = 2023, and the bank as 0 = west and 1 = east. CI = 95% Wald confidence interval.

Predictor	Estimate (β)	Standard Error	z-Value	*p*-Value	95% CI (Lower)	95% CI (Upper)
Intercept	3.30	0.37	8.97	<0.001	2.58	4.02
Year (2023 vs. 2019)	−1.19	0.51	−2.32	0.021	−2.20	−0.18
Bank (East vs. West)	−1.64	0.69	−2.37	0.018	−2.99	−0.28
Soil_PC1	0.37	0.12	3.02	0.003	0.13	0.62
Soil_PC2	0.12	0.18	0.70	0.484	−0.22	0.47

Table 4. Coefficients of the negative binomial generalized linear model (GLM) for *Morus alba* stem counts per plot and year. The response variable is the number of *M. alba* individuals per plot in each sampling year. Explanatory variables are year (2023 vs. 2019), bank (East vs. West), and the first two soil principal components (Soil_PC1 and Soil_PC2), as described in Tables 2 and 3. Estimates (β) are on the log scale, with year coded as 0 = 2019 and 1 = 2023, and bank as 0 = west and 1 = east. CI = 95% Wald confidence interval.

Predictor	Estimate (β)	Standard Error	z-Value	*p*-Value	95% CI (Lower)	95% CI (Upper)
Intercept	−1.08	0.67	−1.62	0.105	−2.39	0.22
Year (2023 vs. 2019)	0.58	0.74	0.79	0.431	−0.87	2.04
Bank (East vs. West)	1.01	0.87	1.15	0.249	−0.70	2.72
Soil_PC1	−0.47	0.18	−2.55	0.011	−0.83	−0.11
Soil_PC2	−0.48	0.31	−1.55	0.121	−1.09	0.13

3.7. Community-Weighted Ellenberg-Type Indicator Values

The community-weighted mean (CWM) Ellenberg-type values for soil moisture (F), nutrients (N) and reaction/pH (R) showed marked temporal shifts between 2019 and 2023 (Table 5). In 2019, the mean CWM_F across plots was 6.28 ± 0.71 (mean ± SD), indicating communities were dominated by species typical of fresh to moderately wet soils, whereas in 2023 the mean CWM_F increased to 7.07 ± 1.36, i.e., towards species associated with wetter conditions. The mean CWM_N remained high and stable between years (6.25 ± 0.41 in 2019 vs. 6.30 ± 0.33 in 2023), reflecting a consistent affinity to nutrient-rich sites. In contrast, the mean CWM_R decreased from 6.74 ± 0.28 to 6.56 ± 0.39, suggesting a slight shift from strongly base-rich species towards more moderately acidic to weakly basic indicator species.

Table 5. Community-weighted Ellenberg-type indicator values, Shannon diversity and invasive abundance per year.

Year	CWM_F Mean ± SD	CWM_N Mean ± SD	CWM_R Mean ± SD	Shannon H′ Mean ± SD	* Invasive Abundance (Individual Plot^{-1}) Mean ± SD
2019	6.28 ± 0.71	6.25 ± 0.41	6.74 ± 0.28	1.01 ± 0.43	94.3 ± 183.2
2023	7.07 ± 1.36	6.30 ± 0.33	6.56 ± 0.39	1.20 ± 0.29	38.4 ± 50.1

* Invasive abundance = *Acer negundo* + *Amorpha fruticosa* + *Morus alba* individuals per plot–year.

The linear mixed effects models confirmed a significant temporal increase in CWM_F (year effect for 2023 vs. 2019: +0.79 ± 0.31; $p = 0.010$), whereas no significant temporal change was detected for CWM_N (+0.05 ± 0.09 and $p = 0.63$; Table 6). CWM_R decreased significantly between 2019 and 2023 (−0.18 ± 0.08 and $p = 0.025$; Table 6). These patterns were consistent across most plots: CWM_F increased in nine out of ten plots (by +0.33 to +2.04 indicator units), while CWM_R decreased in nine out of ten plots (by −0.02 to −0.64 units), indicating consistent directional trends across the study area.

Correlations between the CWM values and soil principal components were generally weak. Across the plots and years, CWM_F and CWM_N were not significantly correlated with the major soil PCA axes ($|r| \leq 0.17$, $p > 0.48$, for Soil_PC1 and Soil_PC2 in all cases), indicating that the within-site variation in Ellenberg-type moisture and nutrient optima of the woody community was largely decoupled from the between-plot edaphic gradients captured by Soil_PC1 and Soil_PC2. Similarly, CWM_R showed only weak, non-significant relationships with Soil_PC1 and Soil_PC2 ($r = -0.18$ and 0.16, respectively; $p > 0.43$).

Table 6. Linear mixed effects models testing temporal changes in community-weighted Ellenberg-type indicator values between 2019 and 2023.

Response	* Intercept (2019) ± SE	Year 2023 Effect ± SE	** *p* (Year 2023)	*** Plot Random Variance	**** Residual Variance	N Plots	N Samples
CWM_F	6.28 ± 0.34	+0.79 ± 0.31	0.010	0.71	0.46	10	20
CWM_N	6.25 ± 0.12	+0.05 ± 0.09	0.634	0.10	0.04	10	20
CWM_R	6.74 ± 0.11	−0.18 ± 0.08	0.025	0.09	0.03	10	20

* Intercept = estimated mean CWM value for 2019. ** Year 2023 effect = difference between 2023 and 2019 (positive values indicate an increase, negative values a decrease). *** Plot random variance = variance of the random intercept, representing spatial differences among plots. **** Residual variance = residual variance within plots/years.

In contrast, there was a tendency for higher CWM_F in more diverse plots: CWM_F was positively correlated with Shannon diversity (H′; $r = 0.44$, $p = 0.055$), whereas CWM_N and CWM_R showed no clear relationships with H′ ($|r| \leq 0.24$, $p > 0.30$). Community-weighted indicator values were not significantly related to the abundance of invasive woody species (*Acer negundo*, *Amorpha fruticosa*, and *Morus alba*; $|r| \leq 0.18$ and $p > 0.44$), suggesting that the main shifts in Ellenberg-type optima reflect broader compositional changes rather than simple responses to the decrease in invaders alone.

3.8. Soil Properties

Tables 7 and 8 show the parameter values of the control (all plants) and the treatments (cutting *A. fruticosa*). All soils are sandy loam with a low percentage of clay. Since no significant differences were detected in the soil properties between the treatment and the control plots (one-way ANOVA; $p > 0.05$), samples from the two groups were pooled and treated as a single dataset (plot–control pooled samples) for subsequent Pearson correlation analysis ($N = 40$). Pearson correlation analysis (Table 9) showed that the Shannon plant diversity index was positively related mainly to soil total organic C, total N, exchangeable K, exchangeable Ca and clay percentage (Supplementary Table S27). Overall, the soil results suggest that edaphic conditions contribute to local variation in woody plant diversity, even though the short-term effects of invasive woody species’ removal on soil properties were not detectable within the timeframe of the study.

https://doi.org/10.3390/land15020335

Table 7. Soil properties in the plots (control).

	pH	$CaCO_3$ (%)	Org. C (%)	Tot N (g/kg)	C/N	Sand (%)	Clay (%)	Silt (%)	Conductivity (µS/cm)	Exch. Ca (meq/100 g)	Exch. Mg (meq/100 g)	Exch. K (meq/100 g)	Exch. Na (meq/100 g)
Average	7.61	1.66	1.25	1.55	8.33	63.5	9.14	27.4	901	16.2	1.01	0.151	0.204
CV (%)	6	71	69	64	37	28	47	50	44	48	127	107	94
Range	6.81–8.30	0.77–3.39	0.2–2.8	0.25–3.5	1.41–12.7	33.3–96.6	2–17.3	1.36–49.4	347–1600	0.25–26.0	0.18–4.33	0.03–0.58	0.02–0.67

Table 8. Soil properties in the plots (treatment: cutting of *A. fruticosa*).

	pH	$CaCO_3$(%)	Org. C (%)	Tot N (g/kg)	C/N	Sand (%)	Clay (%)	Silt (%)	Conductivity (µS/cm)	Exch. Ca (meq/100 g)	Exch. Mg (meq/100 g)	Exch. K (meq/100 g)	Exch. Na (meq/100 g)
Average	7.2	1.51	1.65	1.97	8.13	57.2	10.6	32.2	1011	19.8	0.93	0.166	0.131
CV (%)	9	65	49	43	34	31	50	41	46	41	95	152	95
Range	6.16–8.30	0.52–3.13	0.20–2.8	1.09–3.89	1.84–2.70	29.3–86.6	3.64–21.3	9.72–49.4	414–1773	7.2–31.5	0.16–2.92	0.03–0.86	0.02–0.35

Table 9. Pearson correlation coefficients of soil properties with the Shannon diversity index in plot–control pooled samples.

Soil Properties	Shannon Diversity Index
pH	0.52
$CaCO_3$	0.77 *
Org. C	0.73 *
N	0.76 *
C/N	0.32
Sand	0.66 *
Clay	0.74 *
Silt	−0.57
Conductivity	0.68 *
Ca	0.66 *
Mg	0.46
Ca/Mg	0.33
K	0.62 *
Na	0.52

* Denotes significance level at 0.05 probability levels.

4. Discussion

4.1. Woody Species Diversity and Stand Dynamics in a Mediterranean 91E0 Forest*

This study combined repeated measurements in permanent plots with community-weighted indicator values, functional diversity metrics and invasion modelling to evaluate the short-term dynamics of the priority habitat 91E0* alluvial forests of the Nestos River. Overall, the woody layer remained dominated by native riparian tree and shrub species, and plot-level diversity indices changed only modestly between 2019 and 2023, despite the widespread occurrence of established alien trees and shrubs. At the same time, a marked decline in *Amorpha fruticosa* individuals was documented (from 233 to 142, ~39% reduction) as well as a weaker decrease in *Acer negundo*, indicating that targeted control can substantially reduce the abundance of the main invasive alien taxa without immediately altering plot-level taxonomic diversity. These results suggest that the Nestos alluvial forest is still functionally resilient, but already undergoing a subtle transition towards increasingly invaded and spatially heterogeneous communities.

According to Landon [29], the values of the soil parameters indicate low organic C and exchangeable K. Electrical conductivity is within a range not considered hazardous for plants. The low concentrations of $CaCO_3$ (Tables 7–9) likely reflect the formation of secondary carbonates through the precipitation of carbonate salts in the soil rather than a carbonate-rich parent material. The low values of K in soils should be interpreted together with plant tissue K concentrations. Because this element contributes to plant protection against adverse abiotic factors [37], its uptake from soils warrants dedicated investigation under local site conditions. The total N was relatively high. As no differences were detected between the soil's N concentrations after the removal of *A. fruticosa*, we assume that there is another source of N in the forest, namely alder (*Alnus* sp.) plants abundant in riparian forests, which create symbioses with the actinobacteria Frankia capable of fixing atmospheric N_2.

Previous work in the same habitat has characterized the Nestos alluvial forest as a structurally complex and species-rich riparian system, with *Alnus glutinosa* forming the backbone of the canopy and co-occurring with *Populus alba*, *P. nigra*, *Salix alba* and a diverse shrub layer [38]. Using a larger plot network, Korakaki et al. [38] reported 17 tree and tall shrub species (13 families), and high regeneration indices for both native and alien woody species, with particularly alarming values for *A. fruticosa* and *A. negundo* in 2019.

Our re-measurement of a subset of these permanent plots confirms the overall picture of a structurally diverse riparian forest, but shows that species richness and evenness at the plot scale remained relatively stable over four years, even though individual species' abundances changed.

The persistence of moderate alpha diversity and balanced Shannon and Simpson indices across years suggests that, at least in the short term, the woody assemblage maintains a relatively high degree of redundancy and buffering capacity. Similar patterns have been reported from other European riparian and temperate forests, where compositional change over a decade can be substantial while standard diversity metrics remain comparatively constant because species are replaced by ecologically similar taxa [39]. In the Nestos forest, this buffering likely reflects the dominance of a small set of riparian tree species with overlapping ecological niches and the continued recruitment of both native and alien pioneers in canopy gaps.

Compared with the recent assessment of woody species dynamics in the broader 91E0* area, which focused primarily on stand structure and growth rates in 2023 [40], the present analysis adds an explicitly temporal and multi-metric perspective. By tracking the same plots between 2019 and 2023 and integrating taxonomic, functional and indicator-based metrics, we demonstrate that short-term changes in species composition and invader abundance can occur without an immediate collapse of local woody diversity indices. This nuance is highly relevant for conservation reporting under Article 17 of the Habitats Directive, which increasingly calls for indicators that are sensitive to early degradation but can still distinguish reversible fluctuations from long-term regime shifts [41].

4.2. Invasion Dynamics of Amorpha Fruticosa and Acer Negundo

The Nestos alluvial forest has been identified as one of the Greek hotspots for woody alien plants, with *A. fruticosa* and *A. negundo* showing very high regeneration indices in 2019 and raising concern for the conservation status of habitat 91E0* [38]. Our results confirm that both species remain firmly established in the woody layer, but they also provide important evidence that targeted management can change their local abundance. The ~39% reduction in *A. fruticosa* individuals between 2019 and 2023, as well as the weaker decline in *A. negundo*, are consistent with the manual removal and cutting campaigns implemented under the LIFE PRIMED project, which primarily targeted shrub and sapling stages in this habitat [38].

Given the documented ecological impacts of invasive alien plants, monitoring alone is unlikely to prevent biodiversity and structural degradation unless coupled with sustained control, containment and follow-up actions. This is consistent with the EU Invasive Alien Species framework (Regulation (EU) No 1143/2014), which foresees restrictions and requires early detection/rapid eradication and management measures for listed species of Union concern; notably, *Ailanthus altissima* is included in the Union list.

At a broader spatial scale, *A. fruticosa* is recognized as one of the most problematic invasive shrubs in European riparian systems, with high propagule pressure, strong resprouting ability and a capacity to dominate river banks and floodplains of the Danube and other major rivers [42,43]. Studies from the lower Danube indicate that this species easily colonizes various alluvial habitats, especially showing high invisibility in open, periodically disturbed stands [42]. Climate and land use change projections, moreover, suggest that much of south-eastern Europe, including Greece, will remain climatically suitable or even increasingly favourable for *A. fruticosa* in the coming decades [43]. Against this background, the decline observed in our permanent plots is encouraging but should be interpreted as a local response to sustained removal rather than a spontaneous retreat.

Acer negundo is likewise a widely distributed invasive tree in European riparian and urban forests. In urban riparian corridors in Poland, *A. negundo* dominance has been shown to reduce native woody species richness, homogenize understory vegetation and negatively affect recreation potential [44]. In our study, *A. negundo* remained one of the most prevalent woody species through both survey years, but its abundance decreased slightly. Its distribution was obviously determined by the river bank site and plot category. Conversely, the weaker response by *A. negundo* to management is consistent with its greater height, rapid growth rate and efficient long-distance dispersal making ongoing control more challenging [39,44].

Negative binomial GLMMs found a significant trend in the decrease in invader abundance with time for *A. fruticosa*, and less pronounced but still significant in *A. negundo*. The spatial distribution was affected by the gradient of river bank and site environment factors. This confirms and supports the wider body of evidence indicating that invasive woody species are generally able to respond as a group to hydrological regimes, soil status and history of disturbance [39,41]. Our developmental data add to the genetic and regeneration studies from Avramidou et al. [45], who reported the high genetic diversity and vigorous regeneration of *A. fruticosa* at the same habitat. They show, however, that some components of this regenerative capacity can be mitigated at least locally without immediately depressing woody alpha diversity.

The slight rise in *M. alba* from 2019 to 2023 indicates that it is more of ecologically tolerant or persistent compared to an aggressively invasion-tending species. *M. alba* is highly adaptable to edaphic conditions and can tolerate flooding in riparian areas, as evidenced by natural vegetative regeneration. Bird and non-avian seed dispersal, and proximity to human habitation may assist with local recruitment. The competitive exclusion or suppression of native riparian taxa was not observed for the species in plots. This pattern thus suggests local naturalization with appropriate site conditions, not rapid spreading invasion.

4.3. Beta Diversity, Turnover and Spatial Structuring

The decomposition of between-plot dissimilarity into turnover and nestedness components revealed that beta diversity in the Nestos alluvial forest is dominated by species replacement rather than by systematic species loss. The Sørensen-based total beta diversity was moderate, whereas the Simpson turnover component clearly exceeded the nestedness-resultant component, indicating that plots mainly differ by species substitutions rather than by subsets of a common species pool. This pattern corresponds to the conceptual framework proposed by Baselga [16], who emphasized that high turnover combined with low nestedness often reflects strong small-scale environmental heterogeneity and historical contingencies, rather than a simple gradient of degradation.

In our case, ordination and PERMANOVA detected statistically significant differences in community composition between sampling years and between river banks, but these factors together explained only a modest fraction of the total variation. The east–west separation in PCoA space, combined with the relatively weak correlation of plot-level turnover with the measured soil axes, suggests that unmeasured microtopographic and hydrological factors (e.g., distance to active channels and inundation frequency) and local disturbance events (tree falls and selective cutting) contribute substantially to compositional heterogeneity. The similar dominance of turnover over nestedness has been observed in the alien tree invasions of temperate forests, where invaders frequently encourage spatially diverse mixtures of residual specialists and generalists instead of a strictly nested degradation sequence [39].

From a conservation perspective, the prevalence of turnover implies that maintaining a network of plots across both river banks and capturing the full microhabitat gradient are crucial for representing the gamma diversity of the habitat. It also means that short-term monitoring based solely on species richness or a small set of "diagnostic" species may overlook important shifts in species identities that could have functional consequences. By explicitly quantifying turnover and nestedness, this study provides a more nuanced baseline for tracking whether ongoing management leads to homogenisation (declining turnover) or to a restoration of fine-scale heterogeneity [46].

4.4. Indicator Values and Functional Diversity as Early Warning Tools

Using the harmonized Ellenberg-type indicator values for European vascular plants [23], we derived community-weighted means for light, moisture, reaction and nutrients. These CWMs confirmed that the woody layer is characterized by species adapted to moist, base-rich and moderately nutrient-rich conditions, which is consistent with the ecological definition of habitat 91E0* and with previous vegetation surveys in the Nestos Delta [38]. Between 2019 and 2023, the shifts in mean indicator values were small, and their variation was more strongly associated with soil-related axes and the river bank than with the sampling year. This suggests that, over the study period, the realized ecological niche of the woody layer remained largely stable, despite changes in invader abundance.

Functional diversity indices, including Rao's quadratic entropy and functional dispersion, likewise showed only subtle changes between years and no evidence for a directional erosion of functional space. This result resonates with recent studies showing that invasive trees can substantially modify species composition while leaving functional or phylogenetic diversity largely unchanged, because invaders often occupy trait spaces similar to those of native pioneers and generalists [39]. In the Nestos forest, the combination of stable functional dispersion and moderate compositional turnover indicates that species replacements have so far occurred predominantly within a relatively constrained trait space.

The present work is, to our knowledge, among the first to apply the new European-wide Ellenberg-type indicator dataset of Tichý et al. [23] to a Mediterranean riparian Natura 2000 habitat and to integrate these indicator-based metrics with invasion and beta-diversity analyses. This integration is particularly relevant for journals such as Land that focus on linking field-based ecological information with land use planning and ecosystem service assessments: community-weighted indicator values and functional diversity indices are readily interpretable by managers and can be combined with remote sensing products and hydrological data to build spatially explicit risk indicators for habitat degradation [41].

4.5. Innovation Relative to Previous Work

In the context of the existing literature on habitat 91E0* and on invasive woody species in European riparian systems, this study advances knowledge in several ways:

1. Permanent plots re-measured after targeted invader control. Earlier studies in the Nestos alluvial forest characterized stand structure and regeneration in a single year (either 2019 or 2023) [38,40], examined radial growth characteristics in relation to climate on the east and west banks (providing vegetation strategic management insights) [41], or focused on the genetics and regeneration of *A. fruticosa* alone [47]. Here, we re-measured permanent plots over four years, explicitly spanning a period of active removal of invaders, and quantified how community composition, invader abundance, and diversity metrics jointly responded. This design directly addresses a gap highlighted in global meta-analyses calling for more before–after or removal-based evaluations of invasive plant impacts [42,48].

2. Simultaneous assessment of taxonomic, functional and indicator-based diversity. While the impacts of invasive trees on alpha and beta diversity are increasingly studied [39], few works combine these taxonomic metrics with harmonized Ellenberg-type indicator values and functional dispersion for the woody layer. By doing so, we show that short-term invasion dynamics can substantially reshape species composition and relative abundances while leaving functional diversity and indicator profiles comparatively stable, a pattern that is highly relevant for conservation assessment frameworks that are still predominantly taxon centric.
3. Explicit decomposition of beta diversity into turnover and nestedness in a Mediterranean 91E0* forest. Partitioning beta diversity into its turnover and nestedness-resultant components has become standard in biogeographical studies [16] but has rarely been applied to Mediterranean riparian forests under simultaneous pressures from hydrological alteration and invasion. Our finding that turnover clearly dominates nestedness suggests that conservation strategies must preserve spatial heterogeneity and local environmental gradients, rather than focusing solely on preventing richness loss.
4. Bridging local field data with EU-level policy needs. Finally, by grounding our indicators in harmonized European datasets and by working in a Natura 2000 priority habitat, this study directly supports recent calls to better quantify how invasive alien plants affect conservation status across the network [42,48].

4.6. Implications for Conservation and Potential Applications

The documented decline of *Amorpha fruticosa* and the weaker but detectable reduction in *Acer negundo* further support the effectiveness of targeted management in reducing the abundance of dominant invasive alien woody species, even though short-term changes in plot-level diversity indices remain limited. However, the persistence of both invaders and the strong spatial structuring of communities caution against complacency. For policy and management, our results can be exploited in several ways:

- Refining Natura 2000 monitoring protocols. Community-weighted indicator values and functional diversity metrics can complement traditional structural and compositional indicators in Article 17 reporting, providing early warning signals of hydrological change (via moisture and nutrient CWMs) or incipient biotic homogenization (via declining functional dispersion) even when species richness appears stable [23,42].
- Designing spatially explicit invasive species control. The clear differences between river banks and plot types, together with the dominance of turnover, suggest that management should be stratified by bank and microhabitat. Combining our plot-based metrics with high-resolution land cover data from the Nestos area [38,40] would allow managers to prioritize zones where invader removal is likely to have the greatest biodiversity benefit, or where functional redundancy is low and native species replacement would be particularly harmful.
- Supporting hydro-morphological restoration and land use planning. Our indicator and function-based baseline can be used to calibrate scenarios of altered flooding regime, groundwater abstraction or land use change in the wider delta. For example, projected increases in drought frequency or further bank stabilization could be translated into shifts in Ellenberg moisture CWMs, and thus into expected changes in species composition and invader performance [44].
- Transferability to other 91E0* and riparian systems. The methodological framework permanent plots, invader abundance gradients, beta diversity partitioning and Ellenberg-based CWMs can be readily applied to other alluvial forests in the Balkans and beyond. This would help build a comparative network of sites where

the ecological impacts of invasive woody species on priority habitats are quantified in a harmonized way, as advocated by European assessments of invasive alien plant impacts on Natura 2000 habitats [42,48].

4.7. Future Research

Future work should be implemented in the study area, as presented below:

1. Extend the monitoring to additional survey years to capture longer-term trajectories and the potential lagged effects of invasion and control. This is particularly important for perennial woody species, whose demographic responses and community reassembly may occur over longer time frames; therefore, longer-term resurveys would provide a more robust evidence base for management decision-making and Natura 2000 conservation planning.
2. Combine herb-layer and bryophyte data, as invasive trees and shrubs can substantially affect understory diversity and productivity.
3. Although the present study focused exclusively on the woody layer, it is well established that invasive woody species can indirectly affect understory vegetation (herbaceous plants and bryophytes) through altered light availability, nutrient competition and changes in litter inputs. The absence of systematic understory data therefore represents a limitation of this study, and future monitoring efforts should explicitly integrate herb layer and bryophyte surveys to achieve a more comprehensive assessment of ecosystem-level biodiversity responses in habitat 91E0*.
4. Pair plot-level indicators with detailed hydrological and geomorphological variables, such as distance to channels, inundation frequency, and groundwater levels.
5. Examine socio-ecological factors such as recreation and cultural ecosystem services, particularly given evidence that *A. negundo* can reduce recreational quality in riparian landscapes.

Nonetheless, the integration of multiple years of data from plots, models of the abundance of invading species, beta diversity partitioning, and indicator metrics yield an extensive and policy-relevant perspective on the 91E0* alluvial forests of the Mediterranean and their responses to hydro-morphological regulation and the presence of invasive woody species.

5. Conclusions

This study provides one of the first temporally explicit assessments of woody plant diversity, invasive species dynamics and soil–vegetation relationships in the priority habitat 91E0* alluvial forests of the Nestos River. By re-measuring permanent plots over a four-year interval that coincided with the targeted control of alien woody plants, we were able to disentangle short-term compositional and functional responses of the woody layer to both invasion and management.

First, the woody assemblages remained dominated by native riparian tree and shrub species, and plot-scale taxonomic and functional diversity indices showed only modest variation between 2019 and 2023. This indicates a degree of short-term functional resilience of the habitat, even though species identities and relative abundances changed. The stability of community-weighted Ellenberg-type indicator values further suggests that the realized ecological niche of the woody layer has so far remained compatible with the ecological requirements of habitat 91E0*.

Second, the substantial decrease in *A. fruticosa* and the weaker but significant decrease in *A. negundo* abundance suggest that locally reintensive control of invasive woody plants can suppress these invasive woody species without immediately reducing native woody diversity. Meanwhile, both species, albeit spreading at different rates, remain well established in the system, indicating that continued and more spatially targeted management will be required to curtail their effects on regeneration processes and habitat structure.

Third, beta diversity analyses revealed that compositional differences among plots and between years, are driven predominantly by species turnover rather than simple species loss. This pattern reflects strong fine-scale environmental heterogeneity and microhabitat differentiation between river banks. It also implies that conservation strategies and monitoring designs must capture spatial variation across the full environmental gradient, rather than relying on a small number of plots or solely on species richness metrics.

Fourth, the joint use of community-weighted indicator values and functional diversity indices proved to be a powerful, management-relevant extension of traditional taxonomic descriptors. These integrative metrics are readily interpretable, can be linked to hydrological and soil conditions, and offer a promising early warning framework for detecting subtle shifts in habitat quality, even when taxonomic diversity appears stable.

Overall, the Nestos alluvial forest currently retains key structural and functional attributes of the priority habitat 91E0*, despite ongoing pressures from invasive woody species and hydro-morphological alteration. The short-term resurvey of permanent plots demonstrated that targeted management actions can reduce the abundance of dominant invasive taxa without the immediate loss of native woody diversity or functional heterogeneity. The integrated monitoring framework applied here combining permanent plots, invasion metrics, beta diversity partitioning and indicator-based approaches provides a robust and transferable basis for supporting Article 17 reporting, guiding spatially explicit invasive species management and informing conservation planning in Mediterranean alluvial forests.

Supplementary Materials: The following supporting information can be downloaded at: https://www.mdpi.com/article/10.3390/land15020335/s1. Table S1: List of woody plant species recorded in the study area, including family, biogeographical status, chorology, and life form. Tables S2–S21: Woody plant species composition per permanent plot (P1–P10) for 2019 and 2023. Table S22: Woody plant diversity metrics for all permanent plots in 2019 and 2023, including species richness (S), Shannon diversity (H), Simpson diversity (1-D), and Pielou's evenness (J). Different lowercase letters indicate statistically significant differences between sampling years within plots ($p < 0.05$). Table S23: Rao's quadratic entropy (Rao's Q), percentage of nitrogen-fixing individuals (% N-fix), and percentage of alien individuals (% alien) per plot and year (2019 and 2023). Table S24: Functional dispersion (FDis) values per plot and year (2019 and 2023). Table S25: Trait matrix used for the calculation of functional diversity indices (Rao's Q and FDis), including species origin, life form, nitrogen-fixing ability, and binary coding. Table S26: Eigenvalues and explained variance of the soil principal component analysis (PCA) based on standardized soil variables. Table S27: Loadings of soil variables on the first two principal components (PC1 and PC2) of the soil PCA.

Author Contributions: Conceptualization, A.D.S. and E.K.; methodology, A.D.S., E.K., P.M. and G.K.; software, A.D.S.; validation, A.D.S., E.K., P.M. and G.K.; formal analysis, A.D.S. and P.M.; investigation, A.D.S., E.K., P.M. and G.K.; resources, A.D.S., E.K. and P.M.; data curation, A.D.S., E.K. and P.M.; writing—original draft preparation, A.D.S., E.K., C.G. and P.M.; writing—review and editing, A.D.S., E.K., C.G., P.M. and G.K.; visualization, A.D.S.; supervision, A.D.S.; project administration, E.K.; and funding acquisition, E.K. All authors have read and agreed to the published version of the manuscript.

Funding: This work was supported by the EU LIFE Programme (LIFE PRIMED; grant agreement LIFE17 NAT/GR/000511) and co-financed by the Greek Green Fund.

Data Availability Statement: The data presented in this study are available on request from the corresponding author to maintain privacy.

Acknowledgments: The authors gratefully acknowledge the staff of the Forest Service of Kavala and the Management Unit of Nestos–Vistonida and Rhodope National Parks (N.E.C.C.A.) for their valuable support in planning conservation activities and facilitating fieldwork. We also thank the General Directorate for Forests and Forest Environment of the Hellenic Ministry of Environment and Energy for issuing the research permit. The authors are grateful to the personnel of the Institute of Mediterranean Forest Ecosystems (IMFE), ELGO-DIMITRA, for their assistance with laboratory work. Finally, we acknowledge the Herbarium of the Institute of Mediterranean Forest Ecosystems (Head: Alexandra D. Solomou) for providing biodiversity information and reference material.

Conflicts of Interest: The authors declare no conflicts of interest.

References

1. Naiman, R.J.; Décamps, H. The Ecology of Interfaces: Riparian Zones. *Annu. Rev. Ecol. Syst.* **1997**, *28*, 621–658. [CrossRef]
2. Ward, J.V. The Four-Dimensional Nature of Lotic Ecosystems. *J. N. Am. Benthol. Soc.* **1989**, *8*, 2–8. [CrossRef]
3. Poff, N.L.; Allan, J.D.; Bain, M.B.; Karr, J.R.; Prestegaard, K.L.; Richter, B.D.; Sparks, R.E.; Stromberg, J.C. The Natural Flow Regime. *BioScience* **1997**, *47*, 769–784. [CrossRef]
4. Bendix, J.; Hupp, C.R. Hydrological and Geomorphological Impacts on Riparian Plant Communities. *Hydrol. Process.* **2000**, *14*, 2977–2990. [CrossRef]
5. Tabacchi, E.; Correll, D.L.; Hauer, R.; Pinay, G.; Planty-Tabacchi, A.M.; Wissmar, R.C. Development, Maintenance and Role of Riparian Vegetation in the River Landscape. *Freshw. Biol.* **1998**, *40*, 497–516. [CrossRef]
6. Nilsson, C.; Svedmark, M. Basic Principles and Ecological Consequences of Changing Water Regimes: Riparian Plant Communities. *Environ. Manag.* **2002**, *30*, 468–480. [CrossRef]
7. Merritt, D.M.; Scott, M.L.; Poff, N.L.; Auble, G.T.; Lytle, D.A. Theory, Methods and Tools for Determining Environmental Flows for Riparian Vegetation: Riparian Vegetation—Flow Response Guilds. *Freshw. Biol.* **2010**, *55*, 206–225. [CrossRef]
8. Abernethy, B.; Rutherfurd, I.D. The Distribution and Strength of Riparian Tree Roots in Relation to Riverbank Reinforcement. *Hydrol. Process.* **2001**, *15*, 63–79. [CrossRef]
9. Peterjohn, W.T.; Correll, D.L. Nutrient Dynamics in an Agricultural Watershed: Observations on the Role of a Riparian Forest. *Ecology* **1984**, *65*, 1466–1475. [CrossRef]
10. Junk, W.J.; Bayley, P.B.; Sparks, R.E. The Flood Pulse Concept in River-Floodplain Systems. In *Proceedings of the International Large River Symposium (LARS)*; Dodge, D.P., Ed.; Canadian Special Publication of Fisheries and Aquatic Sciences; Department of Fisheries and Oceans: Ottawa, ON, Canada, 1989; Volume 106, pp. 110–127.
11. Council Directive 92/43/EEC of 21 May 1992 on the Conservation of Natural Habitats and of Wild Fauna and Flora (Habitats Directive). *Official Journal L 206*, 22 July 1992. Available online: https://eur-lex.europa.eu/eli/dir/1992/43/oj/eng (accessed on 15 December 2025).
12. European Commission (DG Environment). *Interpretation Manual of European Union Habitats—EUR28 (April 2013)*; European Commission: Brussels, Belgium, 2013. Available online: https://cdr.eionet.europa.eu/help/natura2000/Documents/Int_Manual_EU28.pdf (accessed on 15 December 2025).
13. Bakker, J.P.; Olff, H.; Willems, J.H.; Zobel, M. Why do we need permanent plots in the study of long-term vegetation dynamics? *J. Veg. Sci.* **1996**, *7*, 147–156. [CrossRef]
14. Kapfer, J.; Hédl, R.; Jurasinski, G.; Kopecký, M.; Schei, F.H.; Grytnes, J.-A. Resurveying historical vegetation data—Opportunities and challenges. *Appl. Veg. Sci.* **2017**, *20*, 164–171. [CrossRef]
15. Legendre, P. A temporal beta-diversity index to identify sites that have changed in exceptional ways in space—Time surveys. *Ecol. Evol.* **2019**, *9*, 3500–3514. [CrossRef] [PubMed]
16. Baselga, A. Partitioning the turnover and nestedness components of beta diversity. *Glob. Ecol. Biogeogr.* **2010**, *19*, 134–143. [CrossRef]
17. Tatsumi, S.; Iritani, R.; Cadotte, M.W. Temporal changes in spatial variation: Partitioning the extinction and colonisation components of beta diversity. *Ecol. Lett.* **2021**, *24*, 1063–1072. [CrossRef] [PubMed]
18. Verheyen, K.; Bažány, M.; Chećko, E.; Chudomelová, M.; Closset-Kopp, D.; Czortek, P.; Decocq, G.; de Frenne, P.; de Keersmaeker, L.; García, C.E.; et al. Observer and relocation errors matter in resurveys of historical vegetation plots. *J. Veg. Sci.* **2018**, *29*, 812–823. [CrossRef]
19. Ross, L.C.; Woodin, S.J.; Hester, A.; Thompson, D.B.A.; Birks, H.J.B. How important is plot relocation accuracy when interpreting re-visitation studies of vegetation change? *Plant Ecol. Divers.* **2010**, *3*, 1–8. [CrossRef]

20. European Environment Agency (EEA); European Topic Centre on Biodiversity and Ecosystems (ETC BE). Guidelines on Concepts and Definitions: Article 17 of Directive 92/43/EEC (Reporting Period 2019–2024); Final Version (June 2023). Available online: https://cdr.eionet.europa.eu/help/habitats_art17/Reporting2025/Final%20Guidelines%20Art.%2017_2019-2024.pdf (accessed on 15 December 2025).
21. European Commission. Proposal for a Regulation of the European Parliament and of the Council on a Monitoring Framework for Resilient European Forests; COM(2023) 728 Final. Brussels, 22 November 2023. Available online: https://environment.ec.europa.eu/system/files/2023-11/COM_2023_728_1_EN_ACT_part1_v8.pdf (accessed on 12 December 2025).
22. Schaffers, A.P.; Sýkora, K.V. Reliability of Ellenberg Indicator Values for Moisture, Nitrogen and Soil Reaction: A Comparison with Field Measurements. *J. Veg. Sci.* **2000**, *11*, 225–244. [CrossRef]
23. Tichý, L.; Axmanová, I.; Dengler, J.; Guarino, R.; Jansen, F.; Midolo, G.; Nobis, M.P.; Van Meerbeek, K.; Aćić, S.; Attorre, F.; et al. Ellenberg-type indicator values for European vascular plant species. *J. Veg. Sci.* **2023**, *34*, e13168. [CrossRef]
24. Dafis, S. *The Forests of Greece*; The Goulandris Natural History Museum: Thessaloniki, Greece, 2010; 192p.
25. Solomou, A.D.; Korakaki, E.; Avramidou, E.; Koulelis, P.; Mantakas, G.; Karetsos, G. Regeneration Status and Diversity of Woody Plant Species in the Priority Habitat 91E0* in Nestos, Greece. *Proceedings* **2025**, *117*, 22. [CrossRef]
26. United Nations Environment Programme (UNEP). *World Atlas of Desertification*, 2nd ed.; Middleton, N., Thomas, D.S.G., Eds.; Arnold: London, UK, 1997; 182p.
27. Proutsos, N.; Korakaki, E.; Bourletsikas, A.; Karetsos, G.; Tsagari, K.; Georgiadis, C. 50-year precipitation trends in Nestos Delta—Natura 2000 site. In Proceedings of the 16th International Conference on Environmental Science and Technology (CEST2019), Rhodes, Greece, 4–7 September 2019. [CrossRef]
28. Bouyoucos, G.J. A Recalibration of the Hydrometer Method for Making Mechanical Analysis of Soils. *Agron. J.* **1951**, *43*, 434–438. [CrossRef]
29. Landon, J.R. (Ed.) *Booker Tropical Soil Manual: A Handbook for Soil Survey and Agricultural Land Evaluation in the Tropics and Subtropics*; Booker Agriculture International Ltd.: London, UK; Longman: New York, NY, USA, 1984.
30. Walkley, A. A Critical Examination of a Rapid Method for Determining Organic Carbon in Soils—Effect of Variations in Digestion Conditions and of Inorganic Soil Constituents. *Soil Sci.* **1947**, *63*, 251–264. [CrossRef]
31. Jones, J.B., Jr. *Laboratory Guide for Conducting Soil Tests and Plant Analysis*; CRC Press: Boca Raton, FL, USA, 2001. [CrossRef]
32. Ibanez, J.J.; De-Alba, S.; Bermudez, F.F.; Garcia-Alvarez, A. Pedodiversity: Consepts and measures. *Catena* **1995**, *24*, 215–232. [CrossRef]
33. Nur, N. *A Statistical Guide to Data Analysis of Avian Monitoring Programs*; BTP-R6001; U.S. Department of the Interior, Fish and Wildlife Service: Washington, DC, USA, 1999.
34. Seaby, R.M.; Henderson, P.A. *Species Diversity and Richness, Version 4*; Pisces Conservation Ltd.: Lymington, UK, 2006.
35. R Core Team. *R: A Language and Environment for Statistical Computing*; R Foundation for Statistical Computing: Vienna, Austria, 2022. Available online: https://www.R-project.org/ (accessed on 30 December 2025).
36. IBM Corp. *IBM SPSS Statistics for Windows, Version 26.0*; IBM Corp.: Armonk, NY, USA, 2019. Available online: https://www.ibm.com/products/spss-statistics (accessed on 10 December 2025).
37. Wang, M.; Zheng, Q.; Shen, Q.; Guo, S. The Critical Role of Potassium in Plant Stress Response. *Int. J. Mol. Sci.* **2013**, *14*, 7370–7390. [CrossRef]
38. Korakaki, E.; Koulelis, P.; Solomou, A.; Karetsos, G.; Proutsos, N.; Avramidou, E.; Kaoukis, K.; Ioannidis, K.; Georgiadis, C. Woody Species Composition, Stand Structure and Growth Dynamics of the Habitat 91E0* Alluvial Forest in Nestos, Greece. In *Recent Advances in Environmental Science from the Euro-Mediterranean and Surrounding Regions*, 3rd ed.; Ksibi, M., Turan, V., Naddeo, V., Hentati, O., Arfi, R.B., Negm, A., Comino, J.R., Khouni, I., Rafatullah, M., Ongoma, V., Eds.; Springer: Cham, Switzerland, 2024; pp. 735–737. [CrossRef]
39. Dyderski, M.K.; Jagodziński, A.M. Impact of Invasive Tree Species on Natural Regeneration Species Composition, Diversity, and Density. *Forests* **2020**, *11*, 456. [CrossRef]
40. Korakaki, E.; Koulelis, P.P.; Solomou, A.D.; Avramidou, E.V.; Karetsos, G.; Mantakas, G.; Kaoukis, K.; Georgiadis, C.; Chatzipavlis, N. Woody Species Dynamics in the Priority Habitat 91E0* in Nestos, Greece. *Proceedings* **2025**, *117*, 28. [CrossRef]
41. Koulelis, P.P.; Avramidou, E.; Korakaki, E.; Solomou, A. Radial Growth Characteristics and Climate on the East and West Banks of the Nestos River, Greece: Vegetation Strategic Management Insights. *Proceedings* **2025**, *117*, 19. [CrossRef]
42. Lazzaro, L.; Bolpagni, R.; Buffa, G.; Gentili, R.; Lonati, M.; Stinca, A.; Lastrucci, L. Impact of Invasive Alien Plants on Native Plant Communities and Natura 2000 Habitats: State of the Art, Gap Analysis and Perspectives in Italy. *J. Environ. Manag.* **2020**, *274*, 111140. [CrossRef]
43. Pedashenko, H.P.; Apostolova, I.I.; Vassilev, K.V. Amorpha fruticosa invasibility of different habitats in lower Danube. *Phytol. Balc.* **2012**, *18*, 285–291.

44. Lapin, K.; Dyderski, M.K. Expanding Range of the Invasive Shrub Amorpha fruticosa under Changing Climate. *Reg. Environ. Change* **2024**, *24*, 152. [CrossRef]
45. Sikorska, D.; Sikorski, P.; Archiciński, P.; Chormański, J.; Hopkins, R.J. You Can't See the Woods for the Trees: Invasive Acer negundo L. in Urban Riparian Forests Harms Biodiversity and Limits Recreation Activity. *Sustainability* **2019**, *11*, 5838. [CrossRef]
46. Legendre, P. Interpreting the replacement and richness difference components of beta diversity. *Glob. Ecol. Biogeogr.* **2014**, *23*, 1324–1334. [CrossRef]
47. Avramidou, E.V.; Korakaki, E.; Malliarou, E.; Solomou, A.D.; Mantakas, G.; Karetsos, G. First Report and Genetic Analysis of the Invasive Species *A. fruticosa* L. in Greece: A Combined Genetic and Regeneration Study. *Ecologies* **2023**, *4*, 627–635. [CrossRef]
48. Vilà, M.; Espinar, J.L.; Hejda, M.; Hulme, P.E.; Jarošík, V.; Maron, J.L.; Pergl, J.; Schaffner, U.; Sun, Y.; Pyšek, P. Ecological Impacts of Invasive Alien Plants: A Meta-Analysis of Their Effects on Species, Communities and Ecosystems. *Ecol. Lett.* **2011**, *14*, 702–708. [CrossRef] [PubMed]